Contents lists available at ScienceDirect

Chemical Engineering Research and Design

journal homepage: www.elsevier.com/locate/cherd

Optimal design of shale gas supply chain network considering MPC-based pumping schedule of hydraulic fracturing in unconventional reservoirs

Yuchan Ahn[a,b], *Prashanth Siddhamshetty*[a,b], *Kaiyu Cao*[a,b], *Jeehoon Han*[c,d], *Joseph Sang-Il Kwon*[a,b,*]

[a] *Artie McFerrin Department of Chemical Engineering, Texas A&M University, College Station, TX, United States*
[b] *Texas A&M Energy Institute, Texas A&M University, College Station, TX, United States*
[c] *School of Chemical Engineering, Chonbuk National University, Jeonju, Republic of Korea*
[d] *School of Semiconductor and Chemical Engineering, Chonbuk National University, Jeonju, Republic of Korea*

ARTICLE INFO

Article history:
Received 23 March 2019
Received in revised form 3 May 2019
Accepted 7 May 2019
Available online 16 May 2019

Keywords:
Shale gas
Hydraulic fracturing
Model predictive control
Supply chain network
Fracture geometry
MILP

ABSTRACT

Several approaches have been developed to design shale gas supply chain network (SGSCN) in an economically viable manner, but the connection between hydraulic fracture geometry, shale gas production, and wastewater recovery has not received much attention. Specifically, the final fracture geometry in unconventional reservoirs significantly affects shale gas production rate and it indirectly determines the amount of recovered wastewater. To take into account the relations among hydraulic fracturing jobs, wastewater generation and management, and shale gas production and management, we focus on the development of a novel framework that integrates a model predictive control (MPC)-based pumping schedule of hydraulic fracturing and a SGSCN model. Based on this developed framework, the optimal SGSCN configuration, which maximizes the overall profit, is determined by solving a mixed-integer linear programming problem. The proposed SGSCN design framework is compared to the case when the same SGSCN model is integrated with a suboptimal pumping schedule like Nolte's pumping schedule. The overall profit of the former is 4.49% higher than that of the latter.

Published by Elsevier B.V. on behalf of Institution of Chemical Engineers.

1. Introduction

Natural gas is one of the most important energy sources in the United States. Currently, 30% of the United States natural gas production is supplied by processing shale gas, which has been enabled by the recent advances in horizontal drilling and hydraulic fracturing technologies (Allen et al., 2013; Howarth et al., 2011; Kargbo et al., 2010; Paltsev et al., 2011; Wang et al., 2014). The amount of shale gas produced from a shale well is determined by the final fracture geometry (i.e., the one at the end of pumping) which is related to the amount of injected freshwater and proppant (Siddhamshetty et al., 2018a). As hydraulic fracturing requires a huge amount of water resources, the profit generated by the extraction of shale gas accompanies environmental concerns, particularly many water-related issues. Furthermore, since shale gas is a hydrocarbon mixture mainly consisting of methane (Administration, 2011), it requires additional processing units for its subsequent use. Therefore, it is very important to understand the supply chain of water consumption and shale gas production; the integrated process that acquires raw materials, and delivers the final products to the markets (Beamon, 1998).

Shale gas supply chain network (SGSCN) consists of two major parts: (1) water network for ensuring the supply of freshwater required for hydraulic fracturing in shale wells and treatment of wastewater generated during shale gas production; (2) shale gas network for separating and storing natural gas, and generating electricity, which is the main consumer of natural gas. Several approaches have been devel-

* *Corresponding author at*: Artie McFerrin Department of Chemical Engineering, Texas A&M University, College Station, TX, United States.
E-mail address: kwonx075@tamu.edu (J.S.-I. Kwon).

https://doi.org/10.1016/j.cherd.2019.05.016
0263-8762/Published by Elsevier B.V. on behalf of Institution of Chemical Engineers.

Nomenclature

Sets

c Centralized wastewater treatment (CWT)
d Disposal well
i Shale site
k Transportation mode
m Power plant
n Number of hydraulic fracturing job
o Onsite treatment
p Processing plant
pi Pipeline capacity
pr Processing plant capacity
s Freshwater source
t Time period of shale gas supply chain network (SGSCN)
tp Time period of shale gas production rate
u Underground reservoir

Parameters

$acdw_i$ Freshwater consumption for each hydraulic fracturing job at shale site i [bbl/well] [1 bbl = 42 gallon = 158.97 liter]
$capc^{pipe}_{pi}$ Capital cost of the pipeline with capcity pi [$]
$capc^{pro}_{pr}$ Capital cost of the processing plant with capacity pr [$]
$ccsw_i$ Correlation coefficient between the amounts of wastewater generated and shale gas produced at shale site i [bbl/mcf] [1 mcf = 1000 ft^3 = 28.32 m^3]
$CEPCI^{pipe}$ Chemical engineering plant cost index (CEPCI) for pipelines [−]
$CEPCI^{pro}$ CEPCI for processing plants [−]
$disr$ Discount rate per each time period
$dis^1_{s,i}$ Distance between freshwater source s and shale site i [mile] [1 mile = 1.61 km]
$dis^2_{i,c}$ Distance between shale site i and CWT facility c [mile]
$dis^3_{i,d}$ Distance between shale site i and disposal well d [mile]
$dis^4_{i,p}$ Distance between shale site i and processing plant p [mile]
$dis^5_{p,m}$ Distance between processing plant p and power plant m [mile]
$dis^6_{p,u}$ Distance between processing plant p and underground reservoir u [mile]
$dis^7_{u,m}$ Distance between underground reservoir u and power plant m [mile]
pa^{shale}_{tp} Amount of shale gas produced at shale sites in time period tp under the model predictive control (MPC)-based and Nolte's pumping schedules [mcf/period]
pri^{elec} Selling price of electricity [$/kWh]
$rCEPCI^{pipe}$ CEPCI for pipelines of the reference year [−]
$rCEPCI^{pro}$ CEPCI for processing plants of the reference year [−]
rr^{onsite}_o Recovery ratio of wastewater treated by onsite treatment o [−]
rr^{drill}_i Recovery ratio of wastewater after completing hydraulic fracturing jobs at shale site i [−]
$uc^{acqi}_{s,t}$ Unit cost of freshwater acquired at freshwater source s in time period t [$/bbl]
uc^{CWT}_c Unit cost of CWT facility c for wastewater treatment [$/bbl]
uc^{disw}_d Unit cost of disposal well d for wastewater injection [$/bbl]
$uc^{drill}_{i,t}$ Unit cost for hydraulic fracturing jobs at shale site i in time period t [$/well]
$uc^{NGL\,sto}$ Unit cost of stored natural gas liquids (NGLs) [$/mcf]
uc^{onsite}_o Unit cost of onsite treatment o for wastewater treatment [$/bbl]
uc^{power}_m Unit cost of power plant m for electricity generation [$/mcf]
uc^{pro} Unit processing cost of shale gas [$/mcf]
$uc^{shale\,prod}_{i,t}$ Unit cost for shale gas production at shale site i in time period t [$/mcf]
$uc^{under-i}_u$ Unit cost for natural gas injection at underground reservoir u [$/mcf]
$uc^{under-w}_u$ Unit cost for natural gas withdrawal at underground reservoir u [$/mcf]
$ucapc^1_{s,i,k}$ Unit transportation capital cost of freshwater between source s and shale site i via transportation mode k [$/mile]
up^{NGL}_t Unit selling price of NGLs in time period t [$/mcf]
$utcc^{CWT}_{i,c,k}$ Unit capital cost of transportation mode k for wastewater supply between shale site i and CWT facility c [$/mile]
$utcc^{disw}_{i,d,k}$ Unit capital cost of transportation mode k for wastewater supply between shale site i and disposal well d [$/mile]
$uvct^{fresh}_k$ Unit variable cost of transportation mode k for freshwater [$/(bbl mile)]
$uvct^{pi-n}$ Unit variable cost of pipeline transportation for natural gas [$/(mcf mile)]
$uvct^{pi-s}$ Unit variable cost of pipeline transportation for shale gas [$/(mcf mile)]
$uvct^{waste}_k$ Unit variable cost of transportation mode k for wastewater [$/(bbl mile)]

Continuous variables

$C^{CWT-tra}$ Transportation cost of CWT facility [$]
$C^{CWT-tre}$ Treatment cost of CWT facility [$]
$C^{disw-inj}$ Injection cost of disposal well [$]
$C^{disw-tra}$ Transportation cost of disposal well [$]
C^{fre-ac} Acquisition cost of freshwater from freshwater sources [$]
C^{fre-tr} Transportation cost required delivering the secured freshwater to shale sites [$]
C^{onsite} Treatment cost of onsite treatment facility [$]
$C^{pro-cap}$ Capital cost required to construct of processing plants [$]
C^{pro-ip} Transportation cost of shale gas between shale sites and processing plants [$]
$C^{pro-ope}$ Operating cost of processing plants [$]
C^{pro-pm} Natural gas transportation cost between processing plants and power plants [$]
C^{pro-pu} Natural gas transportation cost between processing plants and underground reservoirs [$]
C^{pro-um} Natural gas transportation cost between underground reservoirs and power plants [$]
$FWD_{i,t}$ Amount of freshwater required at shale site i in time period t [bbl/period]

$FWR_{s,i,k,t}$ Amount of freshwater supplied between freshwater source s and shale site i via transportation mode k in time period t [bbl/period]
$GE_{m,t}$ Amount of electricity generated at power plant m in time period t [kWh/period]
$NTPM_{p,m,t}$ Amount of natural gas transported between processing plant p and power plant m in time period t [mcf/period]
$NTPU_{p,u,t}$ Amount of natural gas transported between processing plant p and underground reservoir u in time period t [mcf/period]
$NTUM_{u,m,t}$ Amount of natural gas transported between underground reservoir u and power plant m in time period t [mcf/period]
Overallprofit Overall profit of the SGSCN [$]
Profit Profit of the SGSCN [$]
$PS_{i,t}$ Amount of shale gas produced at shale site i in time period t [mcf/period]
$PSLS_{p,t}$ Amount of NGLs sold at processing plant p in time period t [mcf/period]
$SA^{NGL}_{p,t}$ Amount of NGLs stored at processing plant p in time period t [mcf/period]
SI^{elec} Income by selling electricity at power plants [$]
SI^{NGL} Income by selling NGLs at processing plants [$]
$STIP_{i,p,t}$ Amount of shale gas transported between shale site i and processing plant p in time period t [mcf/period]
TAEG Total amount of generated electricity from power plants [kWh]
TC^{fre} Freshwater supply cost [$]
TC^{pow} Power plant cost [$]
TC^{pro} Shale gas processing cost [$]
$TC^{pro-tra}$ Natura gas transportation cost [$]
TC^{sha} Shale gas production cost [$]
TC^{sto} Natural gas and NGL storage cost [$]
TC^{wa} Wastewater management cost [$]
TotalCost Total cost of the SGSCN [$]
$WP^{d}_{i,t}$ Amount of wastewater generated after completing hydraulic fracturing jobs at shale site i in time period t [bbl/period]
$WP^{h}_{i,t}$ Amount of wastewater generated during shale gas production at shale site i in time period t [bbl/period]
$WTIC_{i,c,k,t}$ Amount of wastewater transported between shale site i and CWT facility c via transportation mode k in time period t [bbl/period]
$WTID_{i,d,k,t}$ Amount of wastewater transported between shale site i and disposal well d via transportation mode k in time period t [bbl/period]
$WTIO_{i,o,t}$ Amount of wastewater treated by onsite treatment o at shale site i in time period t [bbl/period]

Binary variables
$XT^{1}_{s,i,k}$ 1 if transportation mode k is selected for freshwater transportation between freshwater source s and shale site i; otherwise it is 0
$XT^{2}_{i,c,t}$ 1 if transportation mode k is selected for wastewater transportation between shale site i and CWT c; otherwise it is 0
$XT^{3}_{i,d,k}$ 1 if transportation mode k is selected for wastewater transportation between shale site i and disposal well d; otherwise it is 0
$Y^{PC}_{pr,p}$ 1 if processing plant p with capacity pr is selected; otherwise it is 0
$Y^{pipe-TCP}_{pi,i,p}$ 1 if pipeline capacity pi is selected for natural gas transportation between shale site i and processing plant p; otherwise it is 0
$Y^{pipe-TCPM}_{pi,p,m}$ 1 if pipeline capacity pi is selected for natural gas transportation between processing plant p and power plant m; otherwise it is 0
$Y^{pipe-TCPU}_{pi,p,u}$ 1 if pipeline capacity pi is selected for natural gas transportation between processing plant p and underground reservoir u; otherwise it is 0
$Y^{pipe-TCUM}_{pi,u,m}$ 1 if pipeline capacity pi is selected for natural gas transportation between underground reservoir u and power plant m; otherwise it is 0

Integer variables
$NHF_{i,t}$ Number of hydraulic fracturing jobs at shale site i in time period t [well/period]
$NHF^{sp}_{i,t,tp}$ Number of hydraulic fracturing jobs at shale site i between time period t and tp [well/period]

oped to study the design and operation of SGSCN. Gao and You (2015b) performed a life-cycle economic and environmental study of SGSCN formulating a multi-objective nonconvex mixed-integer non-linear programming (MINLP) problem based on the previous studies (Cafaro and Grossmann, 2014; Gao and You, 2015a; Yang et al., 2014), and the obtained Pareto-optimal frontier revealed the trade-off between the economic and environmental objectives finding the optimal schedule of hydraulic fracturing jobs, the wastewater treatment options, the amounts of shale gas produced, and electricity generated. Guerra et al. (2016) presented a comprehensive optimization framework for SGSCN to maximize the net present value by determining the amount of freshwater required, and the capacities of shale gas pipeline and compressor for transporting shale gas. Chebeir et al. (2017) proposed a two-stage stochastic programming model to consider uncertain market conditions such as prices and demands of natural gas, while determining an optimal SGSCN configuration as well as wastewater treatment options and the capacities of different processing plants and pipelines throughout SGSCN. Chen et al. (2018) presented an inexact multi-criteria decision-making method for dealing with the life cycle optimization of SGSCN under uncertainty in the price of natural gas.

In spite of these efforts, very few of them took into account the significance of the final fracture geometry on the amounts of shale gas produced and wastewater recovered. In hydraulic fracturing, for example, 10% decrease in the desired fracture length can cause 50% decrease in oil and gas production rates (Cipolla et al., 2009; Siddhamshetty et al., 2018b). Furthermore, the amount of wastewater recovered depends on the amount of freshwater injected to create fractures. Therefore, it is important to consider the fracture geometry which impacts the production rate and the amount of wastewater recovered from fractured wells in determining optimal SGSCN configuration. In recent years, various efforts have been made to achieve the desired fracture geometry in hydraulic fracturing by manipulating the pumping schedule via model-based feedback control systems (Economides and Demarchos, 2008; Gu and Hoo, 2014; Yang et al., 2017; Narasingam and Kwon, 2017; Narasingam et al., 2017, 2018; Siddhamshetty et al., 2018a,b,c, 2019; Singh Sidhu et al., 2018). Using the developed pumping schedule, Etoughe et al. (2018) integrated sustainability considerations of post-fracturing processes with a model-based pumping schedule to minimize the total annual cost of a fixed hydraulic fracturing superstructure. However, they focused on wastewater treatment only and the entire SGSCN along with scheduling of hydraulic fracturing jobs was not considered.

Motivated by these considerations, we focus on the development of a novel framework that integrates model predictive control (MPC)-based pumping schedule of hydraulic fracturing and SGSCN; this integrated approach will allow us to achieve a sophisticated understanding of the complex connections among hydraulic fracturing, wastewater generation and management, and shale gas production and management. Therefore, the computed operating strategy, whose feasibility is not constrained by the reliability and availability of data, can be more generally applicable to broader operating conditions. The closed-loop operation of hydraulic fracturing (i.e., MPC-based pumping schedule applied to the high-fidelity simulation of hydraulic fracturing) is used to compute a final fracture geometry and the amount of freshwater used. From these well attributes, the amounts of shale gas produced and wastewater recovered from the well are calculated by the reservoir simulation software called CMG and the empirical models, respectively. This information is passed as inputs to the SGSCN model; there is no feedback from the SGSCN model to the closed-loop operation of hydraulic fracturing.

Section 2 describes the problem statement for this study. Section 3 describes the objective function and constraints considered within an optimization problem for SGSCN. Case studies are presented to demonstrate the superiority of the proposed model in Section 4. The results of the techno-economic analysis using the proposed model are presented in Section 5. Finally, Section 6 presents conclusions.

2. Problem statement

An optimization problem is formulated to determine the optimal configuration of links among sources (freshwater and shale gas supply) and sinks (treatment technologies for wastewater and power plants for electricity generation) in SGSCN. Several technologies used in this study are as follows: hydraulic fracturing; shale gas processing; electricity generation; wastewater management; transportation; storage.

2.1. *Technology overview*

2.1.1. *Hydraulic fracturing*

Hydraulic fracturing is performed to create fractures with a pressurized liquid such as water with added chemicals and proppant (Economides and Nolte, 1989). It begins with creating initial paths for fractures by generating perforations along the wellbore using explosions. Then, the high-pressure fracturing fluid, called pad (mostly water), is injected into the wellbore to break rock formations and to further propagate fractures. Next, the fracturing slurry consisting of water, additives and proppant is injected at a sufficiently high-pressure into the wellbore. The suspended proppants travel along the fracture at the fracturing fluid's velocity, and the remaining proppants form a stable proppant bank because of gravity settling. Once the pumping is stopped, the fractures in the formation will be closed by the natural stress. The remaining fracturing fluid subsequently leaks into the formation, and the proppant is trapped by the closing walls forming a propped fracture. The propped fracture plays a key role to promote the flow of hydrocarbons from the reservoir to the wellbore, and the massive leaking fracturing fluid stimulates the formation. As multiple wells and multiple fractures on each well are generated in the shale site, a large volume of freshwater is required for hydraulic fracturing.

2.1.2. *Shale gas processing*

Shale gas contains higher-order hydrocarbons such as ethane, propane, butane, etc.; they are called natural gas liquids (NGLs) which can be sold in the market to produce valuable by-products or they can be used to generate electricity at power plants. Due to the high market values of NGLs compared to that of natural gas, separation of NGLs from shale gas is necessary.

2.1.3. *Electricity generation*

A gas turbine combined cycle power plant is considered that produces electricity with a 50% efficiency based on the lower heating value determined by subtracting the heat of vaporization of the water from the higher heating value (Weber and Clavin, 2012). Natural gas separated at processing plants is consumed at power plants to generate electricity, which is then sold in the market.

2.1.4. *Wastewater management*

Once hydraulic fracturing is completed, shale gas is produced from the stimulated shale well. At the same time, a fraction of the freshwater injected into the shale well flows back to the surface along with the produced shale gas (Lira-Barragán et al., 2016; Yang et al., 2014). This wastewater contains toxic chemical contaminants such as volatile organic compounds, trimethylbenzenes, and xylenes (Annevelink et al., 2016) which must be handled via proper wastewater management technologies. In this work, three options are considered for the wastewater management as follows: onsite treatment (Bartholomew and Mauter, 2016; Horner et al., 2011; Lutz et al., 2013; Olmstead et al., 2013; Slutz et al., 2012); centralized wastewater treatment (CWT) (Bartholomew and Mauter, 2016; Lutz et al., 2013; Olmstead et al., 2013; Slutz et al., 2012; Wilson and VanBriesen, 2012); disposal well (Bartholomew and Mauter, 2016; Horner et al., 2011; Slutz et al., 2012; Wilson and VanBriesen, 2012). On-site treatment for wastewater can be performed in various ways which includes multi-effect distillation (MED), multi-stage flash (MSF), and reverse osmosis (RO) (Jang et al., 2017; Van der Bruggen and Vandecasteele, 2002). Wastewater treated by the onsite treatment facility can be mixed with freshwater for hydraulic fracturing jobs at a nearby shale site. CWT can be used to treat wastewater without reusing it, and the treated water will be discharged to surface water. Also, wastewater can be transported and pumped down to disposal wells without any further treatment.

2.1.5. *Transportation*

Two transportation modes for SGSCN, truck and pipeline, are considered (Gao and You, 2015b). Freshwater can be transported to a shale site via truck and/or pipeline. Trucks can be used to supply small volume of water, because the water demand for different shale sites varies over time, and the trucks can respond flexibly to these changes (Ahn et al., 2015). On the other hand, shale gas and NGLs can be delivered by pipelines because of a large volume of gas to be transported.

2.1.6. *Storage*

Two storage options, underground reservoir and NGL storage unit, are considered for SGSCN. Natural gas from shale gas processing plants is transported to power plants and underground reservoirs. Underground reservoirs are considered to handle fluctuations in demand and price of electricity, both of which significantly influence the overall profit of SGSCN (Slutz et al., 2012). Separated natural gas can be stored in underground reservoirs for an indefinite period of time before transported to power plants (Gao and You, 2015c) and NGLs also can be immediately sold in the market or stored in NGL storage units and then sold in the market (Gao and You, 2015b).

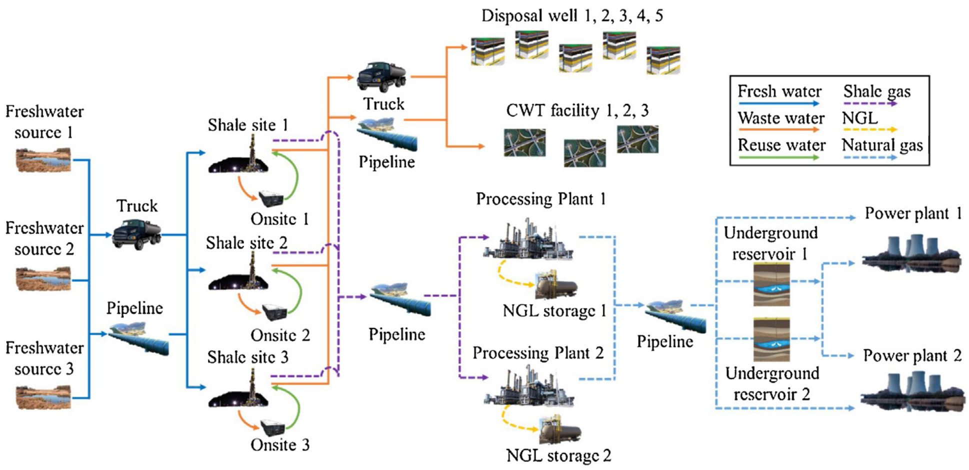

Fig. 1 – SGSCN superstructure.

2.2. MPC-based pumping schedule of hydraulic fracturing

In hydraulic fracturing, it is very important to achieve a uniform proppant bank height and desired fracture geometry as they will lead to the maximum gas production rate. To achieve this objective, we developed a MPC-based pumping schedule design technique for hydraulic fracturing. Specifically, we first constructed a reduced-order model (ROM) using the data from a high-fidelity model of hydraulic fracturing. Then, we developed a Kalman filter to estimate unmeasurable variables using the available measurements such as fracture width at the wellbore and fracture length. Then, we developed a MPC formulation to compute an optimal pumping schedule that will allow us to achieve the above-mentioned objectives.

2.3. SGSCN configuration

A SGSCN pathway represents a typical supply chain network. The objective of this work is to determine the optimal network configuration of SGSCN (Fig. 1) to maximize its economic performance by optimizing the following strategic and operational decisions: (1) amount of freshwater required at each shale site via transportation modes from freshwater sources to shale sites; (2) amount of wastewater generated after hydraulic fracturing jobs at each shale site and wastewater management options; (3) transportation modes from shale sites to CWT facilities or disposal wells; (4) scheduling of multiple hydraulic fracturing jobs and the amount of shale gas produced at each shale site; (5) numbers, capacities, and locations of shale gas processing plants; (6) amount of natural gas stored in each underground reservoir and the amount of NGLs stored in each NGL storage unit; (7) numbers, capacities, and locations of power plants; (8) capacities of pipelines among shale sites, shale gas processing plants, underground reservoirs, and power plants.

SGSCN can be configured as source and sink nodes for the water and shale gas networks. The water network consists of nodes for freshwater sources, shale sites, onsite treatment facilities, disposal wells, and CWT facilities. Source and sink systems of the shale gas network include nodes for the shale sites, processing plants with NGL storage units, underground reservoirs, and power plants. Shale gas produced at each shale site is supplied to processing plants for separation into natural gas and NGLs. The separated NGLs can be immediately sold in the market or stored in NGL storage units and then sold in the market. Also, the natural gas separated at processing plants can be immediately supplied to power plants to produce electricity, or it can be stored in underground reservoirs at the moment and supplied to power plants later.

To our best knowledge, this is the first study that computes the shale gas production rates and the amount of wastewater recovered by utilizing a MPC-based pumping schedule and a reservoir simulator, and applies these results to SGSCN. Schematic representation of the proposed framework is shown in Fig. 2. Specifically, within the proposed MPC-based pumping schedule of hydraulic fracturing, seven important decision variables are determined as follows (Fig. 2): (1) fracture length at each well; (2) fracture width at each well; (3) number of fractures at each well; (4) number of hydraulic fracturing jobs at each shale site; (5) amount of freshwater required at each well; (6) amount of wastewater generated at each well during shale gas production; (7) amount of shale gas produced from each well.

Remark 1. As schematically illustrated in Fig. 2, the values for the output variables obtained by the closed-loop operation of hydraulic fracturing (i.e., MPC-based pumping schedule applied to the high-fidelity model) are used as the inputs to the SGSCN model. For example, the final propped fracture geometry (e.g., fracture width, length and height) at the end of pumping are utilized to predict the amounts of shale gas produced, freshwater required, and wastewater recovered for each well; this data will be considered along with the SGSCN model to determine the optimal operating strategies in water network (e.g., locations of freshwater sources and wastewater treatment options after hydraulic fracturing jobs) and shale gas network (e.g., schedule of hydraulic fracturing jobs and capacities of process plants and power plants) that maximize the overall profit of SGSCN.

3. Model formulation

3.1. MPC-based pumping schedule design technique for hydraulic fracturing

3.1.1. Optimal fracture and well configuration in unconventional reservoirs

In hydraulic fracturing, the required optimal fracture geometry depends on the geological properties of the rock formation. For example, in conventional reservoirs, a wide and short

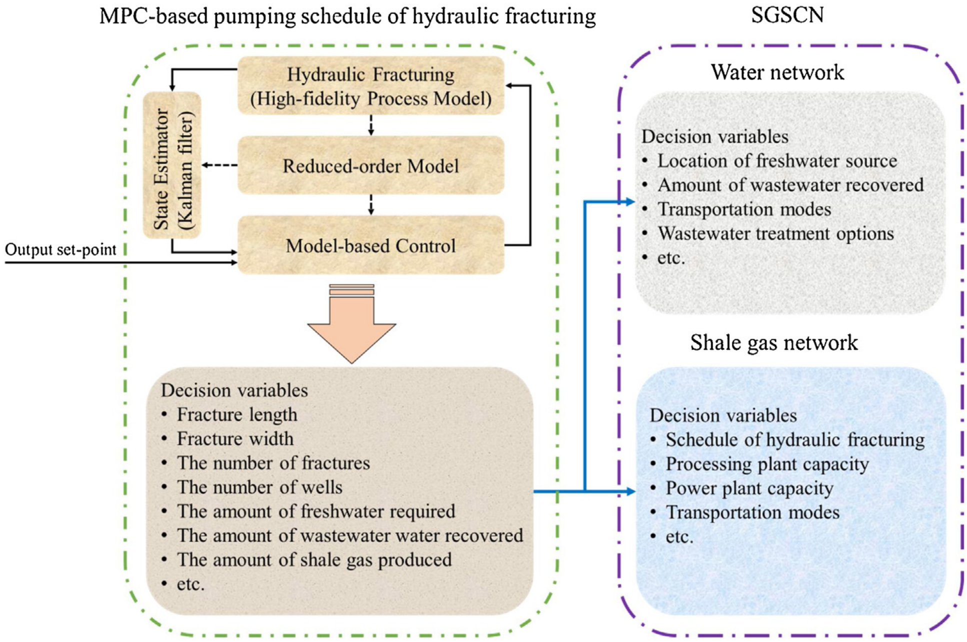

Fig. 2 – Simplified diagram of the proposed MPC-based pumping schedule and SGSCN.

fracture is preferred due to the high-permeability of rock formation, but in unconventional low-permeability shale formations, a narrow and long fracture is preferred (Bhattacharya et al., 2012). Recently, Liu and Valkó (2017) proposed a section-based optimization method, which is an offline optimization-based technique to find the number of wells, n_c, number of fractures per well, n_r, and fracture half-length, x_f, that maximize the shale gas production rate from unconventional shale formations for given amounts of fracturing resources such as the amount of freshwater and proppant to be injected. In this work, the total amount of proppant to be injected is $M_{prop} = 2.38 \times 10^7$ kg, and the optimal decision variables for this proppant using the section-based optimization method are $n_c = 6$, $n_r = 55$, and $x_f = 120$ m. Please refer to (Siddhamshetty et al., 2018a) for more details regarding the section-based optimization method.

In unconventional reservoirs, due to the use of slickwater (i.e., low-viscosity fracturing fluid) the proppant settles quickly forming a proppant bank, which will eventually reach an equilibrium height, h_{eq}. It is very important to achieve this equlibirum height of proppant bank over the required fracture half-length, x_f, which can be translated into achieving the following average fracture width at the end of pumping:

$$W_{avg,\,target} = \frac{M_{prop,frac}}{2\rho_p h_{eq} x_f (1-\emptyset)}. \tag{1}$$

where the total injected proppant per fracture is $M_{prop,frac} = 72{,}000$ kg, the proppant particle density is $\rho_p = 2{,}650$ kg/m^3, the porosity of proppant bank is $\emptyset = 0.61$, the equilibrium height of proppant bank for the considered flow conditions is $h_{eq} = 54$ m, and the calculated average fracture width at the end of pumping is $W_{avg,\,target} = 5.37$ mm.

To achieve the uniform proppant bank height and optimal fracture geometry, it is important to develop a pumping schedule to inject fracturing fluid and proppant. One of the most commonly used pumping schedules is developed by Nolte (1986), which is formulated as follows:

$$C_0(tt) = \begin{cases} C_{target}\left(\frac{tt - tt_p}{tt_e - tt_p}\right)^{\epsilon} & for\, tt \geq tt_p \\ 0 & for\, tt < tt_p \end{cases}. \tag{2}$$

where C_{target} denotes the target proppant concentration, ε is an exponent calculated based on the fracturing fluid efficiency, tt_e is the total pumping time, and tt_p is the pad time during which only clean fluid without proppant is injected. Nolte's pumping schedule has a few practical limitations as follows: (1) proppant settling is not considered; (2) fracturing fluid flowrate is constant and only proppant concentration is varied; (3) plant-model mismatch due to the predefined form of the pumping schedule and open-loop operation may lead to a short propped fracture length.

Remark 2. One of the most commonly used approaches for generating the pumping schedule is developed by Nolte. This approach has been widely used because of its easy-to-implement nature, and it is based on the conservation of fluid volume, particularly estimating the amount of fluid that leaks off during the hydraulic fracturing treatment. Although this approach has some limitations, it is still one of the most widely adopted pumping schedules by many oil and gas companies.

3.1.2. *MPC formulation for optimal pumping schedule*

3.1.2.1. *Reduced order model.* The ROM used in the MPC framework is developed using the closed-loop simulation data of hydraulic fracturing. First, a series of step inputs are applied to the high-fidelity process model to generate input/output data. Then, a linear time-invariant state-space model describing hydraulic fracturing process is obtained using the multivariable output error state-space (MOESP) algorithm, which is presented in the following form:

$$x(t_{k+1}) = Ax(t_k) + Bu(t_k) \tag{3}$$

$$y(t_k) = Cx(t_k) \quad (4)$$

where $u(tt_k) = [Q_{x0}(tt_k), C_0(tt_k)]^T$ is the flow rate and proppant concentration of the fracturing fluids at the wellbore (i.e., the manipulated input variables) and the output variables are $y(tt_k) = [W_{avg}(tt_k), W_0(tt_k), L(tt_k)]^T$ where $W_{avg}(tt_k)$ is the average fracture width, $W_0(tt_k)$ is the fracture width at the wellbore, and $L(tt_k)$ is the fracture length.

3.1.2.2. MPC formulation. To deal with the limitations of Nolte's pumping schedule described in Remark 2, we use the MPC formulation developed by Siddhamshetty et al. (2018a) to achieve the desired average fracture width, $W_{avg,\,target}$, which will lead to a uniform proppant bank height over the optimal fracture half-length at the end of pumping. The MPC is formulated in the following form, which will compute the optimal pumping schedule (flowrate and proppant concentration of fracturing fluid injected at the wellbore) by minimizing the squared deviation of the average fracture width at the end of pumping from its set-point value:

$$\min_{\substack{C_{stage,j},\,\ldots,\,C_{stage,9} \\ Q_{stage,j},\,\ldots,\,Q_{stage,9}}} \left(W_{avg}\left(tt_f\right) - W_{avg,target}\right)^2, \quad (5)$$

$$s.t.\ ROM\ and\ Kalman\ filter, \quad (6)$$

$$\tilde{W}_0\left(tt_j\right) = W_0\left(tt_j\right), \tilde{L}\left(tt_j\right) = L\left(tt_j\right), \quad (7)$$

$$C_{stage,j-1+m} \le C_{stage,j+m} \le 2\,\mathrm{PPGA},\ m = 1, \ldots, 9-j, \quad (8)$$

$$Q_{min} \le Q_{stasge,j+m} \le Q_{max},\ m = 1, \ldots, 9-j, \quad (9)$$

$$\Delta\left(\sum_{j=1}^{9} 2Q_{stage,j}C_{stage,j}\right) = M_{prop,frac}. \quad (10)$$

where the ROM is developed in a manner described in Siddhamshetty et al. (2018a) using the closed-loop simulation data of hydraulic fracturing. In hydraulic fracturing, the available real-time measurements are the fracture width at the wellbore, $W_0\left(tt_j\right)$, and the fracture length, $L\left(tt_j\right)$. These measurements are then used in the Kalman filter to estimate unmeasurable average fracture width, $\hat{W}_{avg}\left(tt_j\right)$, and initial states of the system which will be used in the MPC formulation to predict future state trajectories; the Kalman filter plays a role as a soft sensor to estimate unmeasurable variables at each sampling time. The concentraion unit used in this study is 1 pound of proppant added to one gallon of fluid (PPGA). The pumping schedule, consisting of fracturing fluid flow rate, $Q_{stage,j}$, and proppant concentration $C_{stage,j}$, is obtained by solving the above optimization problem in the shrinking prediction horizon, $N_p = tt_f - tt_j$, where tt_f is the total hydraualic fracturing operation time and tt_j is the current time. In this formulation, we considered the practical constraints on (1) maximum proppant concentration injected, (2) minimum and maximum allowable limits on fracturing fluid flow rate, and (3) the amount of proppant to be injected at the end of pumping. For detailed explaination of the MPC-based pumping schedule of hydraulic fracturing, the readers may refer to Siddhamshetty et al. (2018a).

After we obtain the pumping schedule, the total amount of freshwater injected to each well is caluclated using the following equation:

$$Q_{freshwater} = n_r\Delta\sum_{j=1}^{9} 2Q_{stage,j}\left(1 - C_{stage,j}\right). \quad (11)$$

Remark 3. In this work, we developed a linear time-invariant state-space model using the closed-loop simulation data. This linear state space model was then used in the Kalman filter for state estimation. The training input was designed by taking into account the ranges of allowed input profile (i.e., the minimum and maximum allowable flow rate and proppant concentration). As a result, we implicitly considered the input constraints used in the MPC formulation when developing the ROM and thereby in the Kalman filter. Therefore, in this work, advanced state estimation schemes like moving horizon estimation were not needed because we did not consider any state constraints.

3.2. *Wastewater model*

In this subsection, we developed a dynamic model to predict the flowrate of wastewater generated from each well during shale gas production. The data used to develop this model is taken from Hayes, 2009. Using this data and a regression method, we developed the following equation to predict the flowrate profile of wastewater generated from a well for a given amount of freshwater injected:

$$Q_f(tt) = Q_{freshwater}\left(a\ln(tt) + b\right). \quad (12)$$

where a and b are the parameters determined by a regression method, and $Q_{freshwater}$ is the volume of injected freshwater per each well. In this work, we considered three months as one time period and the recovery ratio of wastewater is calculated using the following equation:

$$rr_i^{drill} = \frac{\sum_{tt=1}^{90} Q_f(tt)\,dt}{Q_{freshwater}}. \quad (13)$$

Remark 4. With the developed dynamic input–output model and the injected freshwater amount determined by pumping schedule, the corresponding cumulative volume of recovered wastewater can be readily available. However, since the input–output model does not affect the hydraulic fracturing process, even if Eq. (12) was considered within the MPC formulation, the obtained pumping schedule would not change.

3.3. *Shale gas production model*

In this work, we use the reservoir simulation software called CMG, developed by Computer Modelling Group Ltd., to predict a shale gas production profile using the final fracture geometry at the end of pumping. Specifically, using the propped fracture geometry as the input, the shale gas production profile per each quarter, pa_{tp}^{shale}, is obtained.

3.4. *SGSCN model*

In this study, the proposed network model is obtained by modifying the previous SGSCN; in particular, the models describing shale gas production rate and the capacities of pipelines and shale gas processing plants have been changed (Gao and You, 2015b). This approach allows determining different decision variables within one framework, which can be formulated using a mixed-integer linear programming (MILP) problem for the strategic and operational design of SGSCN from freshwater sources to electricity generation, simultaneously taking into account technology, resource, and capacity constraints over a multi-site and multi-period planning horizon. This model involves numerous key parameters and variables. The models for objective function and constraints are described below. The readers may refer to the electronic supplemental information (ESI) for additional details regarding the model.

3.4.1. *Objective function*

In this study, the objective is to maximize the overall profit (*Overallprofit*) of the SGSCN which is obtained by subtracting the total cost (*TotalCost*) from the profit (*Profit*) as follows:

$$\mathit{Maximize\,Overallprofit} = \mathit{Profit} - \mathit{TotalCost}. \tag{14}$$

In the SGSCN, there are two products, electricity and NGLs, that are sold externally. *Profit* can be determined by adding the sum of their sales values, given by:

$$\mathit{Profit} = SI^{elec} + SI^{NGL}. \tag{15}$$

where SI^{elec} and SI^{NGL} denote sale incomes of electricity and NGLs, respectively, and SI^{elec} can be calculated by the amount of electricity generated at power plants, given by:

$$SI^{elec} = pri^{elec}\,TAEG$$

where pri^{elec} denotes the selling price of electricity and *TAEG* is the total amount of electricity generated from power plants, given by:

$$TAEG = \sum_{m}\sum_{t} GE_{m,t}. \tag{17}$$

where $GE_{m,t}$ denotes the amount of electricity generated at power plant m in time period t.

Another product produced in the SGSCN is NGLs, which is separated from natural gas at processing plants. SI^{NGL} can be calculated by the amount of NGLs sold at processing plant p ($PSLS_{p,t}$), given by:

$$SI^{NGL} = \sum_{p}\sum_{t} \frac{up_t^{NGL}\,PSLS_{p,t}}{(1+disr)^t}. \tag{18}$$

where up_t^{NGL} denotes the unit selling price of NGLs in time period t and *disr* is the discount rate per time period.

TotalCost, which is another component in the objective function, Eq. (14), includes several costs as follows: (1) freshwater supply cost, TC^{fre}; (2) shale gas production cost, TC^{sha}; (3) wastewater management cost, TC^{wa}; (4) shale gas processing plant cost, TC^{pro}; (5) natural gas transportation cost, $TC^{pro-tra}$; (6) natural gas and NGL storage cost, TC^{sto}; (7) power plant cost, TC^{pow}.

$$\mathit{TotalCost} = TC^{fre} + TC^{sha} + TC^{wa} + TC^{pro} + TC^{pro-tra} + TC^{sto} + TC^{pow}. \tag{19}$$

3.4.1.1. *Freshwater supply cost*. A large amount of freshwater is needed to produce shale gas at each shale site. For the freshwater supply, the acquisition cost of freshwater from freshwater sources, C^{fre-ac}, and the transportation cost required delivering the secured freshwater to shale sites, C^{fre-tr}, have to be considered to account for the total cost, TC^{fre}, associated with fresh water supply, which is given below:

$$TC^{fre} = C^{fre-ac} + C^{fre-tr}. \tag{20}$$

To supply the amount of freshwater required from freshwater sources to shale sites, the acquisition of freshwater is needed, and its cost is proportionally charged to the amount of freshwater acquired.

$$C^{fre-ac} = \sum_{s}\sum_{i}\sum_{k}\sum_{t} \frac{uc_{s,t}^{acqi}\,FWR_{s,i,k,t}}{(1+disr)^t}. \tag{21}$$

where $uc_{s,t}^{acqi}$ denotes the unit acquisition cost of freshwater at freshwater source s in time period t and $FWR_{s,i,k,t}$ is the amount of freshwater supplied between freshwater source s and shale site i via transportation mode k in time period t.

C^{fre-tr} is the freshwater transportation cost, which includes the capital and variable costs of the transportation modes, given by:

$$C^{fre-tr} = \sum_{s}\sum_{i}\sum_{k}\sum_{t}\left(ucapc_{s,i,k}^{1}\,dis_{s,i}^{1}\,XT_{s,i,k}^{1} + \frac{uvct_k^{fresh}\,dis_{s,i}^{1}\,FWR_{s,i,k,t}}{(1+disr)^t}\right). \tag{22}$$

where $ucapc_{s,i,k}^{1}$ is the unit transportation capital cost of freshwater between freshwater source s and shale site i via transportation mode k, $dis_{s,i}^{1}$ is the distance between freshwater source s and shale site i, $XT_{s,i,k}^{1}$ is 1 if transportation mode k is selected for freshwater transportation between freshwater source s and shale site i, and $uvct_k^{fresh}$ is the unit variable cost of transportation mode k for freshwater transportation.

3.4.1.2. *Shale gas production cost*. The shale gas production cost is related to the number of hydraulic fracturing jobs at shale sites and the amount of shale gas produced. TC^{sha} is the total production cost of shale gas, which includes the hydraulic fracturing cost and shale gas production cost from all shale sites, given by:

$$TC^{sha} = \sum_{i}\sum_{t} \frac{uc_{i,t}^{drill}\,NHF_{i,t}}{(1+disr)^t} + \sum_{i}\sum_{t} \frac{uc_{i,t}^{shale\,prod}\,PS_{i,t}}{(1+disr)^t}. \tag{23}$$

where $uc_{i,t}^{drill}$ and $uc_{i,t}^{shale\,prod}$ denote the unit cost for hydraulic fracturing jobs and for shale gas production at shale site i in time period t, respectively, $NHF_{i,t}$ is the number of hydraulic fracturing jobs at shale site i in time period t, and $PS_{i,t}$ is the amount of shale gas produced at shale site i in time period t.

3.4.1.3. *Wastewater management cost*. Once hydraulic fracturing is completed, wastewater is recovered along with shale gas production. The total cost of wastewater management, TC^{wa}, is calculated by considering the followings: (1) transportation cost of CWT facility, $C^{CWT-tra}$; (2) treatment cost of

CWT facility, $C^{CWT-tre}$; (3) transportation cost of disposal well, $C^{disw-tra}$; (4) injection cost of disposal well, $C^{disw-inj}$; (5) total cost of onsite treatment facility, TC^{onsite}.

$$TC^{wa} = C^{CWT-tra} + C^{CWT-tre} + C^{disw-tra} + C^{disw-inj} + C^{onsite}. \quad (24)$$

where $C^{CWT-tra}$ is the transportation cost of CWT facility, which includes the capital and variable costs of the transportation modes selected for CWT as follows:

$$C^{CWT-tra} = \sum_i \sum_c \sum_k \sum_t \left(utcc^{CWT}_{i,c,k}\, dis^2_{i,c}\, XT^2_{i,c,k} + \frac{uvct^{waste}_k\, dis^2_{i,c}\, WTIC_{i,c,k,t}}{(1+disr)^t} \right). \quad (25)$$

where $utcc^{CWT}_{i,c,k}$ denotes the unit capital cost of transportation mode k for the wastewater supply between shale site i and CWT facility c, $dis^2_{i,c}$ is the distance between shale site i and CWT facility c, $XT^2_{i,c,t}$ is 1 if transportation mode k is selected for wastewater transportation between shale site i and CWT facility c, $uvct^{waste}_k$ is the unit variable cost of transportation mode k, and $WTIC_{i,c,k,t}$ is the amount of wastewater transported between shale site i and CWT facility c via transportation mode k in time period t. The wastewater treated by CWT facility is discharged to the surface water.

$C^{CWT-tre}$ is the treatment cost of CWT facility which includes the operating cost considering the amount of transported wastewater:

$$C^{CWT-tre} = \sum_i \sum_c \sum_k \sum_t \frac{uc^{CWT}_c\, WTIC_{i,c,k,t}}{(1+disr)^t}. \quad (26)$$

where uc^{CWT}_c denotes the unit cost of CWT facility c for wastewater treatment.

Another way to handle wastewater is to use the disposal well without any treatment. This disposal well is in general located farther than CWT facilities, so the corresponding transportation cost affects the decision of whether to use this disposal well or not.

$C^{disw-tra}$ is the transportation cost of disposal wells, which includes the capital and variable costs associated with transportation modes for disposal wells, given by:

$$C^{disw-tra} = \sum_i \sum_d \sum_k \sum_t \left(utcc^{disw}_{i,d,k}\, dis^3_{i,d}\, XT^3_{i,d,k} + \frac{uvct^{waste}_k\, dis^3_{i,d}\, WTID_{i,d,k,t}}{(1+disr)^t} \right) \quad (27)$$

where $utcc^{disw}_{i,d,k}$ denotes the unit capital cost of transportation mode k for wastewater supply between shale site i and disposal well d, $dis^3_{i,d}$ is the distance between shale site i and disposal well d, $XT^3_{i,d,t}$ is 1 if transportation mode k is selected for wastewater transportation between shale site i and disposal well d, and $WTID_{i,d,k,t}$ is the amount of wastewater transported between shale site i and disposal well d via transportation mode k in time period t,

$C^{disw-inj}$ is the wastewater injection cost over the entire disposal wells, which is given by:

$$C^{disw-inj} = \sum_i \sum_d \sum_k \sum_t \frac{uc^{disw}_d\, WTID_{i,d,k,t}}{(1+disr)^t}. \quad (28)$$

where uc^{disw}_d denotes the unit cost of disposal well d for wastewater injection.

Onsite treatment reuses wastewater by mixing with freshwater for another hydraulic fracturing job. The distance between shale site and onsite treatment facility is neglected by assuming that onsite treatment facilities are located nearby the shale sites where hydraulic fracturing jobs take place, and C^{onsite} is the onsite treatment cost to reuse wastewater, which is given by:

$$C^{onsite} = \sum_i \sum_o \sum_t \frac{uc^{onsite}_o\, WTIO_{i,o,t}}{(1+disr)^t}. \quad (29)$$

where uc^{onsite}_o denotes the unit cost of onsite treatment o for wastewater treatment and $WTIO_{i,o,t}$ is the amount of wastewater treated by onsite treatment o at shale site i in time period t.

3.4.1.4. Shale gas processing cost. A processing plant is needed for separation of shale gas into natural gas and NGLs. The total cost of processing plant, TC^{pro}, is calculated by considering the followings: capital cost of processing plant, $C^{pro-cap}$; operating cost of processing plant, $C^{pro-ope}$; transportation cost of shale gas between shale sites and processing plants, C^{pro-ip}:

$$TC^{pro} = C^{pro-cap} + C^{pro-ope} + C^{pro-ip}. \quad (30)$$

where $C^{pro-cap}$ depends on the capacities of processing plants as follows:

$$C^{pro-cap} = \sum_{pr} \sum_p capc^{pro}_{pr}\, Y^{PC}_{pr,p} \left(\frac{CEPCI^{pro}}{rCEPCI^{pro}} \right). \quad (31)$$

where $capc^{pro}_{pr}$ denotes the capital cost of the processing plant with capacity pr, $Y^{PC}_{pr,p}$ is 1 if processing plant p with capacity pr is selected, and $CEPCI^{pro}$ and $rCEPCI^{pro}$ are the chemical engineering plant cost index (CEPCI) for processing plants and the CEPCI for processing plants of the reference year, respectively.

$C^{pro-ope}$ is the total operating cost of processing plants, which is given by:

$$C^{pro-ope} = \sum_i \sum_p \sum_t \frac{uc^{pro}\, STIP_{i,p,t}}{(1+disr)^t}. \quad (32)$$

where uc^{pro} denotes the unit processing cost for shale gas and $STIP_{i,p,t}$ denotes the amount of shale gas transported between shale site i and processing plant p in time period t.

C^{pro-ip} is the transportation cost of shale gas via transportation modes between shale sites and processing plants, which includes the capital and operating costs of pipelines, as follows:

$$C^{pro-ip} = \sum_{pi} \sum_i \sum_p capc^{pipe}_{pi}\, Y^{pipe-TCP}_{pi,i,p} \left(\frac{CEPCI^{pipe}}{rCEPCI^{pipe}} \right)$$

$$+\sum_i\sum_p\sum_t \frac{uvct^{pi-s}\,dis^4_{i,p}\,STIP_{i,p,t}}{(1+disr)^t}. \quad (33)$$

where $capc^{pipe}_{pi}$ denotes the capital cost of pipeline with capacity pi, $Y^{pipe-TCP}_{pi,i,p}$ is 1 if pipeline capacity pi is selected for natural gas transportation between shale site i and processing plant p, $uvct^{pi-s}$ is the unit variable cost of pipeline transportation for shale gas, $dis^4_{i,p}$ is the distance between shale site i and processing plant p, and $CEPCI^{pipe}$ and $rCEPCI^{pipe}$ are the CEPCI for pipelines and the CEPCI for pipelines of the reference year, respectively.

3.4.1.5. *Natural gas transportation cost.* Natural gas separated at processing plants is transported to power plants for electricity generation. The total cost of natural gas transportation among processing plants, power plants, and underground reservoirs, $TC^{pro-tra}$, is calculated by considering the followings: distance from processing plants to power plants, C^{pro-pm}; distance from processing plants to underground reservoirs C^{pro-pu}; distance from underground reservoirs to power plants, C^{pro-um}, as follows:

$$TC^{pro-tra} = C^{pro-pm} + C^{pro-pu} + C^{pro-um}. \quad (34)$$

where C^{pro-pm}, C^{pro-pu}, *and* C^{pro-um} are the natural gas transportation costs between processing plants and power plants, between processing plants and underground reservoirs, and between underground reservoirs to power plants, respectively.

$$C^{pro-pm} = \sum_{pi}\sum_p\sum_m \left(capc^{pipe}_{pi}\,Y^{pipe-TCPM}_{pi,p,m}\left(\frac{CEPCI^{pipe}}{rCEPCI^{pipe}}\right)dis^5_{p,m}\right) + \sum_p\sum_m\sum_t \frac{uvct^{pi-n}\,dis^5_{p,m}\,NTPM_{p,m,t}}{(1+disr)^t}, \quad (35)$$

$$C^{pro-pu} = \sum_{pi}\sum_p\sum_u \left(capc^{pipe}_{pi}\,Y^{pipe-TCPU}_{pi,p,u}\left(\frac{CEPCI^{pipe}}{rCEPCI^{pipe}}\right)dis^6_{p,u}\right) + \sum_p\sum_m\sum_t \frac{uvct^{pi-n}\,dis^6_{p,u}\,NTPU_{p,u,t}}{(1+disr)^t}, \quad (36)$$

$$C^{pro-um} = \sum_{pi}\sum_u\sum_m \left(capc^{pipe}_{pi}\,Y^{pipe-TCUM}_{pi,u,m}\left(\frac{CEPCI^{pipe}}{rCEPCI^{pipe}}\right)dis^7_{u,m}\right) + \sum_u\sum_m\sum_t \frac{uvct^{pi-n}dis^7_{u,m}\,NTUM_{u,m,t}}{(1+disr)^t}. \quad (37)$$

where $capc^{pipe}_{pi}$ denotes the capital cost of pipeline with capacity pi, $dis^5_{p,m}$, $dis^6_{p,u}$, and $dis^7_{u,m}$ are the distances between processing plant p and power plant m, between processing plant p and underground reservoir u, and between underground reservoir u and power plant m, respectively, $Y^{pipe-TCPM}_{pi,p,m}$, $Y^{pipe-TCPU}_{pi,p,u}$, and $Y^{pipe-TCUM}_{pi,u,m}$ are 1 if the pipeline is selected for natural gas transportation between processing plant p and power plant m, between processing plant p and underground reservoir u, and between underground reservoir u and power plant m, respectively, $uvct^{pi-n}$ is the unit variable cost of pipeline transportation for natural gas, and $NTPM_{p,m,t}$, $NTPU_{p,m,t}$, and $NTUM_{u,m,t}$ are the amounts of natural gas transported between processing plant p and power plant m, between processing plant p and underground reservoir u, and between underground reservoir u and power plant m, in time period t, respectively.

3.4.1.6. *Natural gas and NGL storage cost.* In this study, two storage options for natural gas and NGLs are considered. Underground reservoirs store natural gas before transporting it to power plants, and storage units are used to store NGLs before selling them in the market. TC^{sto} denotes the total storage cost at underground reservoirs and NGL storage units, which is given below:

$$TC^{sto} = \sum_u\sum_t\left(\frac{\left(\sum_p uc^{under-i}_u\,NTPU_{p,u,t} + \sum_m uc^{under-w}_u\,NTUM_{u,m,t}\right)}{(1+disr)^t}\right) + \sum_p\sum_t \frac{uc^{NGL\,sto}\,SA^{NGL}_{p,t}}{(1+disr)^t}. \quad (38)$$

where $uc^{under-i}_u$ and $uc^{under-w}_u$ denote the unit costs for wastewater injection and withdrawal at underground reservoir u, respectively, $uc^{NGL\,sto}$ is the unit cost of stored NGLs, and $SA^{NGL}_{p,t}$ is the amount of NGLs stored at processing plant p in time period t.

3.4.1.7. *Electricity generation cost.* Finally, electricity is generated by natural gas supplied from processing plants and underground reservoirs. TC^{pow} is the total cost of electricity generation at power plants using natural gas, which is given by:

$$TC^{pow} = \sum_m\sum_t\left(\left(\sum_p NTPM_{p,m,t} + \sum_u NTUM_{u,m,t}\right)\frac{uc^{power}_m}{(1+disr)^t}\right). \quad (39)$$

where uc^{power}_m denotes the unit cost of power plant m for electricity generation.

3.4.2. Constraints

This section presents constraints on the amount of freshwater required, wastewater generated, and shale gas produced.

3.4.2.1. *Freshwater supply.* A huge amount of freshwater is required to make fractures for shale gas production. The amount of freshwater required at shale site i in time period t, $FWD_{i,t}$, is related to the number of hydraulic fracturing jobs at shale site i, as follows:

$$FWD_{i,t} = acdw_i NHF_{i,t},\ \forall i, t. \quad (40)$$

where $NHF_{i,t}$ denotes the number of hydraulic fracturing jobs at shale site i in time period t, and $acdw_i$ denotes the freshwater consumption for each hydraulic fracturing job at shale site i, which is determined by the proposed MPC-based pumping schedule of hydraulic fracturing ($Q_{freshwater}$ in Eqs. (11)–(13)).

Table 1 – Design parameters used in the case studies for SGSCN.

The available number of freshwater sources (Yang et al., 2014)	3
The available number of shale sites (Ladlee and Jacquet, 2011)	3
The available numbers of hydraulic fracturing jobs (Siddhamshetty et al., 2018a)	6
The available number of CWT facilities (Al-Nory et al., 2014; Raluy et al., 2006)	3
Onsite treatment technologies (Al-Nory et al., 2014; Raluy et al., 2006)	MSF, MED, and RO
The available number of processing plants (He and You, 2014)	2
The available number of power plants (Cost, 2014; Weber and Clavin, 2012)	2
The available number of underground reservoirs (Kumar et al., 2017)	2
Transportation modes (Gao and You, 2015b)	Truck and pipeline
Total planning horizon (Cafaro and Grossmann, 2014)	10 years

Furthermore, $FWD_{i,t}$ can be supplied by freshwater sources and reused water from onsite treatment facilities.

$$\sum_{o} rr_{o}^{onsite} WTIO_{i,o,t} + \sum_{s}\sum_{k} FWR_{s,i,k,t} = FWD_{i,t},\ \forall i, t. \tag{41}$$

where rr_{o}^{onsite} denotes the recovery ratio of wastewater treated by onsite treatment o, $WTIO_{i,o,t}$ is the amount of wastewater treated by onsite treatment o at shale site i in time period t, and $FWR_{s,i,k,t}$ is the amount of freshwater supplied between freshwater source s and shale site i via transportation mode k in time period t.

3.4.2.2. *Wastewater generation*. The amount of wastewater generated after completing hydraulic fracturing jobs, $WP^{d}{}_{i,t}$, is related to the number of hydraulic fracturing jobs as follows:

$$WP^{d}{}_{i,t} = acdw_i\, rr_{i}^{drill}\, NHF_{i,t},\ \forall i, t. \tag{42}$$

where rr_{i}^{drill} denotes the recovery ratio of wastewater after completing hydraulic fracturing jobs at shale site i, determined by the proposed MPC-based pumping schedule of hydraulic fracturing (Eq. (13)).

Also, the amount of wastewater generated during shale gas production, $WP_{i,t}^{h}$, is proportional to the total amount of shale gas produced as follows:

$$WP^{h}{}_{i,t} = ccsw_i PS_{i,t},\ \forall i, t. \tag{43}$$

where $ccsw_i$ denotes the correlation coefficient between the amounts of wastewater generated and shale gas produced at shale site i, and $PS_{i,t}$ is the amount of shale gas produced at shale site i in time period t.

The total amount of wastewater generated ($WP^{d}{}_{i,t} + WP^{h}{}_{i,t}$) should equal to the total amount of wastewater handled by the three wastewater management options (CWT, disposal well, and onsite treatment), which is described by:

$$WP^{d}{}_{i,t} + WP^{h}{}_{i,t} = \sum_{o}\sum_{k} WTIO_{i,o,t} + \sum_{c}\sum_{k} WTIC_{i,c,k,t} + \sum_{d}\sum_{k} WTID_{i,d,k,t},\ \forall i, t. \tag{44}$$

where $WTIC_{i,c,k,t}$ and $WTID_{i,d,k,t}$ denote the amount of wastewater transported between shale site i and CWT facility c and between shale site i and disposal well d, respectively, via transportation mode k in time period t.

3.4.2.3. *Shale gas production*. The total amount of shale gas produced from shale sites can be obtained by the production rate of shale gas and the number of hydraulic fracturing jobs at each shale site as follows:

$$\sum_{tp} NHF_{i,t,tp}^{SP}\, pa_{tp}^{shale} = PS_{i,t},\ \forall i, t. \tag{45}$$

where $NHF_{i,t,tp}^{SP}$ is the number of hydraulic fracturing jobs at shale site i between time period t and tp, and pa_{tp}^{shale} is the amount of shale gas produced at shale sites in time period tp under the proposed MPC-based and Nolte's pumping schedules. Details of other constrains for SGSCN are described in ESI.

4. Case study

To illustrate the performance of the proposed model, two case studies were adopted from Gao and You (2015b), which was based on Marcellus shale play. The design parameters used for several facilities of the SGSCN are taken from the literature and are shown in Table 1.

Specifically, Nolte's pumping schedule (Nolte, 1986) and the proposed MPC-based pumping schedule (Siddhamshetty et al., 2018a) are considered in this study. Operation data determined by the proposed MPC-based and Nolte's pumping schedules are shown in Tables S1 and S2 and Fig. S1 in ESI, and they are used in the SGSCN to compare the optimal designs between the two cases based on the following assumption:

1. Produced shale gas is assumed to be a mixture of an ideal gas.
2. Compositions of shale gas and wastewater are assumed to be constant, so they are not considered in this study.
3. Three months are set as one time period, and this model considers for ten years (forty time periods).
4. Hydraulic fracturing operations are completed within one time period.
5. The available number of hydraulic fracturing jobs at each shale site is known beforehand.
6. Shale gas can be extracted once fractures are created via hydraulic fracturing.
7. The amount of shale gas produced in each well decreases with time as represented in Table S1 and Fig. S1 in the ESI.
8. Wastewater is generated during shale gas production and its amount is related to the amount of shale gas produced in each shale site.
9. The capacities of pipelines for resource transportation and processing plants for shale gas separation have to be determined.
10. Electricity produced at power plants and NGLs separated from shale gas in processing plants are sold in the market.

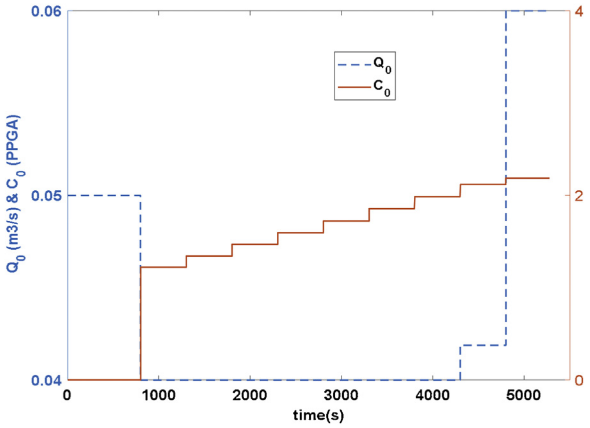

Fig. 3 – Optimal pumping schedule computed by the proposed MPC-based pumping schedule.

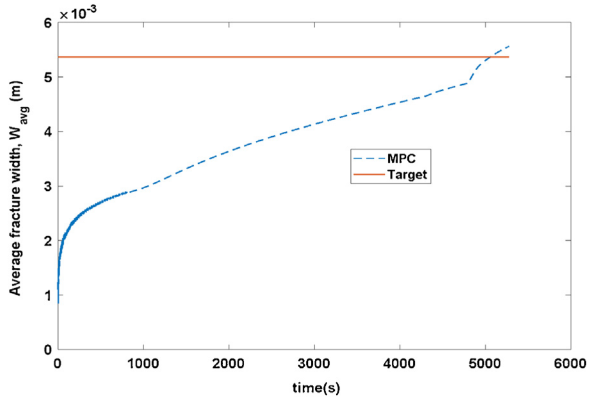

Fig. 4 – Average fracture width profile under the proposed MPC-based pumping schedule.

5. Results and discussion

This section explains how to optimize the SGSCN by taking into account the variables computed by the proposed MPC-based pumping schedule, such as the final fracture geometry at the end of pumping and the amount of freshwater supplied.

5.1. *MPC-based pumping schedule of hydraulic fracturing*

In this section, we apply the proposed MPC-based pumping schedule to regulate the average fracture width at the end of pumping to a desired value, which will lead to a uniform proppant bank height and optimal fracture geometry.

In the closed-loop simulations, the pad time was fixed to be 800 s to avoid premature termination of hydraulic fracturing process, and Δ and tt_f were chosen to be 500 s and 5,300 s, respectively. We divided the pumping schedule into 9 pumping stages with a duration of 500 s for each pumping stage, which was equal to the sampling time, Δ. At the beginning of each pumping stage, the real-time measurements of fracture width at the wellbore, W_0, and the fracture length, L, were utilized as the initial conditions to the ROM. Applying constant flow rate and proppant concentration input values obtained from the proposed MPC framework over a prediction horizon length of $N_p = tt_f - tt_j$, in a sample-and-hold fashion over the entire pumping stage, the ROM is solved with a fixed integration time step of 0.1 s to predict the state and output values. The formulated optimization problem is a linear quadratic problem, and we used a constrained optimized algorithm (fmincon) in MATLAB to solve this optimization problem. The computation time to solve the optimization problem at each sampling time is given in Table S5 in the ESI. Please note all the calculations were performed using MATLAB on a Dell workstation, powered by Intel(R) Core(TM) i7-4790 CPU@3.60 GHz, running the Windows 8 operating system.

The desired average fracture width at the end of pumping is $W_{avg,\,target} = 5.37$ mm. The generated pumping schedule is presented in Fig. 3, and it is observed from Fig. 4 that the average fracture width at the end pumping is close to $W_{avg,\,target}$.

Fig. 5a shows that the proppant bank height is uniform over the required fractures length (i.e., 120 m) compared to Nolte's pumping schedule (Fig. 5b) where the proppant bank height is uniform only until 106.5 m.

According to the proposed MPC-based optimal pumping schedule, the volume of the freshwater required for each fractured well is $V_{freshwater} = 23867.8\,\text{m}^3$, while it was $V_{freshwater} = 26331.8\,\text{m}^3$ under Nolte's pumping schedule. By applying these values to the developed dynamic input–output model, the total amounts of the wastewater for ten years are $V_{wastewater} = 13323.9\,\text{m}^3$ and $V_{wastewater} = 14699.4\,\text{m}^3$ with the proposed MPC-based and Nolte's pumping schedules, respectively. Meanwhile, using the reservoir simulator, CMG, the shale gas production profiles for the two cases were generated based on the corresponding fracture geometry. It can be observed from Table S1 and Fig. S1 in ESI that the total shale gas production using the proposed MPC-based pumping schedule is higher than Nolte's pumping schedule because the former was able to achieve the optimal fracture geometry. The results determined by the proposed MPC-based pumping schedule, such as the amount of freshwater required, wastewater generated, and shale gas produced in each well, are shown in Fig. S1 and Tables S1 and S2.

5.2. *SGSCN model*

The proposed model for the SGSCN was solved using General Algebraic Modeling System (GAMS 24.3.1; CPLEX 12.6) with Intel® Core™ i7-4770 CPU@3.40 GHz and 16 GB RAM, running Windows 10 Enterprise 64bit. The formulated optimization problems include 15,464 continuous variables, 1,138 discrete variables, and 16,739 constraints. A low optimality gap (0.1) was achieved in this model, and two case studies were performed.

5.2.1. *Optimal costs*

The overall profit of the SGSCN (Fig. 6) is determined by comparing two profits (i.e., incomes from selling electricity and NGLs) and seven costs (i.e., freshwater transportation cost, shale gas production cost, wastewater treatment cost, shale gas processing cost, shale gas transportation cost, gas storage cost, and electricity generation cost).

When considering the shale gas production for 10 years, the overall profit of the former (264×10^6 US$), which utilized the proposed MPC-based pumping schedule, was 4.49% higher than that of the latter (252×10^6 US$), which was designed on Nolte's pumping schedule. In both cases, the profits generated by selling electricity whose market price is US$ 0.1215 per kWh Administration (2019), dominate the other part. Another major profit can be achieved by selling NGLs separated from shale gas in the market. The total costs were 198.84×10^6 and 233.85×10^6 US$ for Nolte's and the proposed MPC-based pumping schedules, respectively. Specifically, the processing

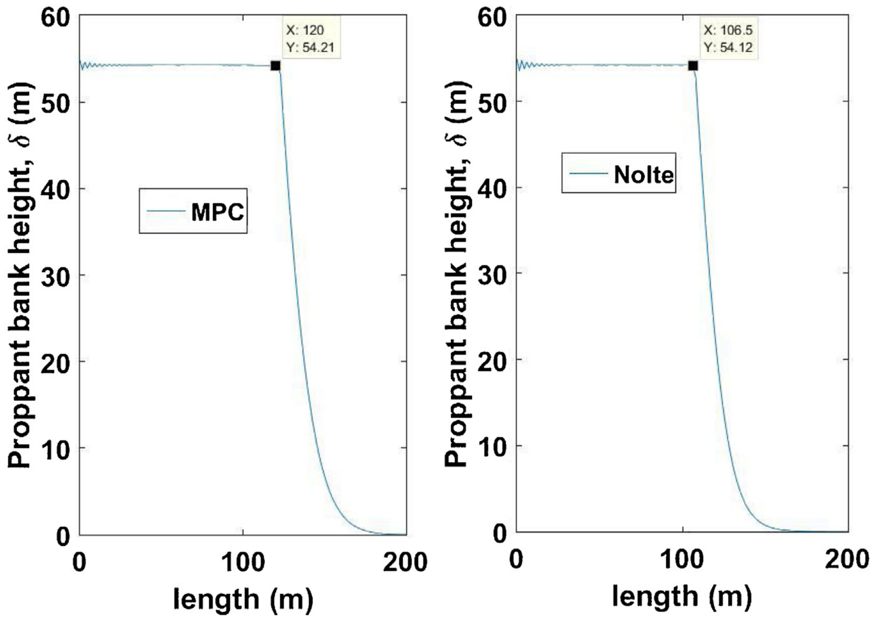

Fig. 5 – Proppant bank height profile obtained at the end of pumping using (a) the proposed MPC-based pumping schedule and (b) Nolte's pumping schedule.

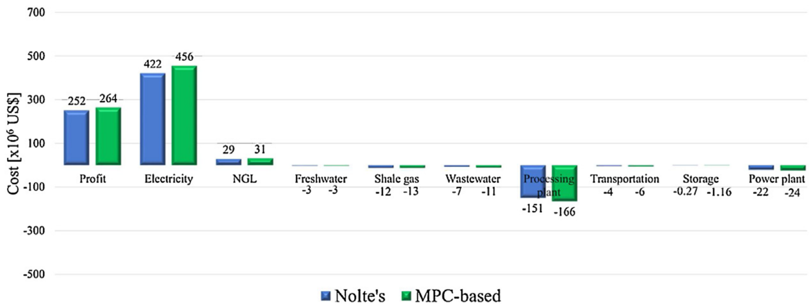

Fig. 6 – Comparison of optimal costs of the SGSCN based on different pumping schedules.

plant costs (151×10^6 and 166×10^6 US$) in both cases were higher than the other costs because the formers included the construction costs of processing plants and the operating costs.

The next highest costs were the power plant costs; 22×10^6 and 24×10^6 US$ for Nolte's and the proposed MPC-based pumping schedules, respectively. These costs include the transportation costs to power plants and the production costs using natural gas. On the other hand, the wastewater cost is significantly different between the two cases. The wastewater treatment cost in the proposed MPC-based pumping schedule (11×10^6 US$) was 57.14% higher than that of Nolte's pumping schedule (7×10^6 US$). This means that different wastewater management options were selected between the two cases. This result is also observed in the optimal SGSCN configurations computed under the two different pumping schedules.

5.2.2. *Optimal network configurations*

With Nolte's pumping schedule, the optimal SGSCN configuration was determined as follows (Fig. 7): two freshwater sources; two shale sites with eleven hydraulic fracturing jobs; two CWT facilities; two shale gas processing plants with two NGL storage units; one underground reservoir; two power plants.

The amounts of freshwater required in the two shale sites were satisfied from freshwater sources by two trucks and one pipeline. The amounts of freshwater transported to shale site 1 is supplied from freshwater sources 1 (810,000 bbl) and 2 (514,979 bbl) by trucks. On the other hand, the freshwater to shale site 2 was supplied (1,104,149 bbl) from freshwater source 2 by a pipeline. To handle the wastewater generated during shale gas production at shale sites, two CWT facilities were selected, and the generated wastewater was transported by trucks. The wastewater from shale site 1 was treated at CWT facility 1 and then discharged to surface water (1,208,132 bbl) and the wastewater from shale site 2 was treated at both CWT facilities 1 (726,577 bbl) and 2 (21,017 bbl). Total eleven hydraulic fracturing jobs were completed over three years in shale sites 1 (six wells) and 2 (five wells). To handle the shale gas produced from the two shale sites, two shale gas processing plants (1,200,000 msf per time period in processing plant 1 and 300,000 msf per time period in processing plant 2) were constructed with two NGL storage units. The produced shale gas was transported to processing plants by pipelines, and the separated natural gas was supplied via pipelines to the two power plants for electricity generation; in particular, the total amount of 1,918,424,456 MW h and 1,552,209,794 MW h were generated from power plants 1 and 2, respectively. The details of the optimal network design in the case of using Nolte's pumping schedule are shown in Table 2.

On the other hand, when the proposed MPC-based pumping schedule is used, the optimal SGSCN configuration was determined as follows (Fig. 8): two freshwater sources; two

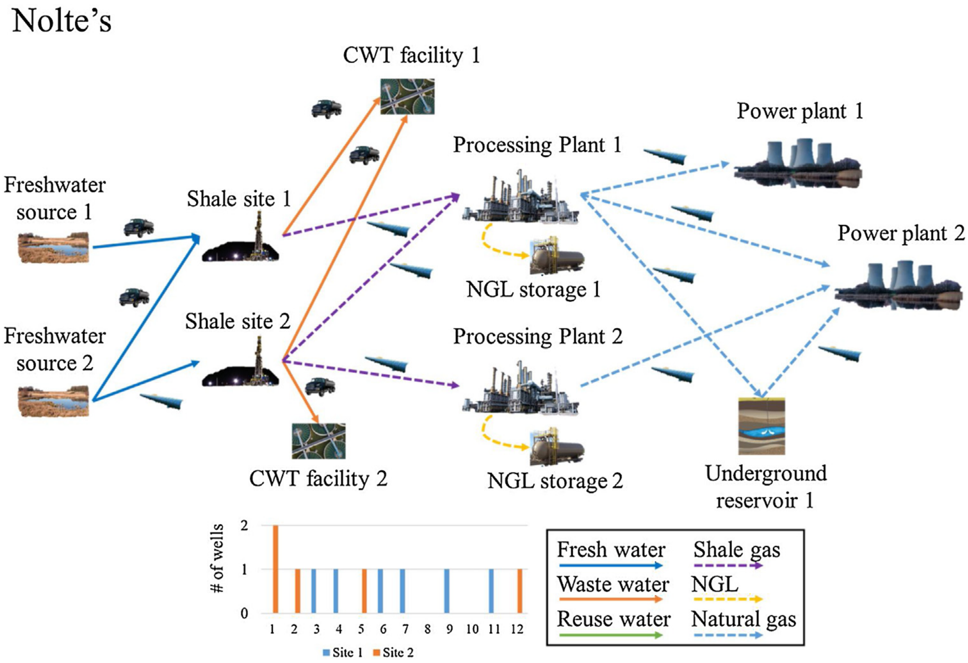

Fig. 7 – Optimal SGSCN configuration when Nolte's pumping schedule is used.

Table 2 – Optimal design results when Nolte's and the proposed MPC-based pumping schedules are used.

		Nolte's	MPC-based	
Total amount of freshwater		2,429,128	2,196,484	bbl
Source 1	Truck	810,000	810,000	
	Pipeline	–	–	
Source 2	Truck	514,979	390,992	
	Pipeline	1,104,149	995,492	
Source 3	Truck	–	–	
	Pipeline	–	–	
Total amount of wastewater		1,955,726	1,993,658	bbl
Site 1	WTC (truck)	1,208,132	–	
	WTD (pipeline)	–	1,261,561	
	WTO	–	–	
Site 2	WTC (truck)	747,594	709,835	
	WTD	–	–	
	WTO	–	22,262	
Site 3	WTC (truck)	–	–	
	WTD	–	–	
	WTO	–	–	
Total amount of shale gas production		30,066,662	32,471,196	mcf
Site 1		16,202,547	17,860,939	
Site 2		13,864,116	14,610,258	
Site 3		–	–	
Total amount of natural gas and NGLs		29,164,663	31,597,061	mcf
Processing plant 1	Natural gas	24,939,047	26,905,113	
	NGL	3,476,510	3,776,788	
Processing plant 2	Natural gas	636,739	733,644	
	NGL	112,366	181,516	
Total amount of natural gas transportation		25,575,787	27,638,757	mcf
Processing plant	Power plant	15,929,394	17,114,373	
	Reservoir	9,646,392	10,524,384	
Underground reservoir	Power plant	9,646,392	10,524,384	
Total electricity generation		3,470,634,250	3,750,579,323	MWh
Power plant 1		1,918,424,456	2,033,137,345	
Power plant 2		1,552,209,794	1,717,441,978	

shale sites with eleven hydraulic fracturing jobs; two processing plants with two NGL storage units; one underground reservoir; two power plants; one onsite treatment facility; one CWT facility; one disposal well.

The amounts of freshwater required in the two shale sites were satisfied from the freshwater sources by trucks. The amount of freshwater transported to shale site 1 is supplied from both freshwater sources 1 (810,000 bbl) and 2 (390,992

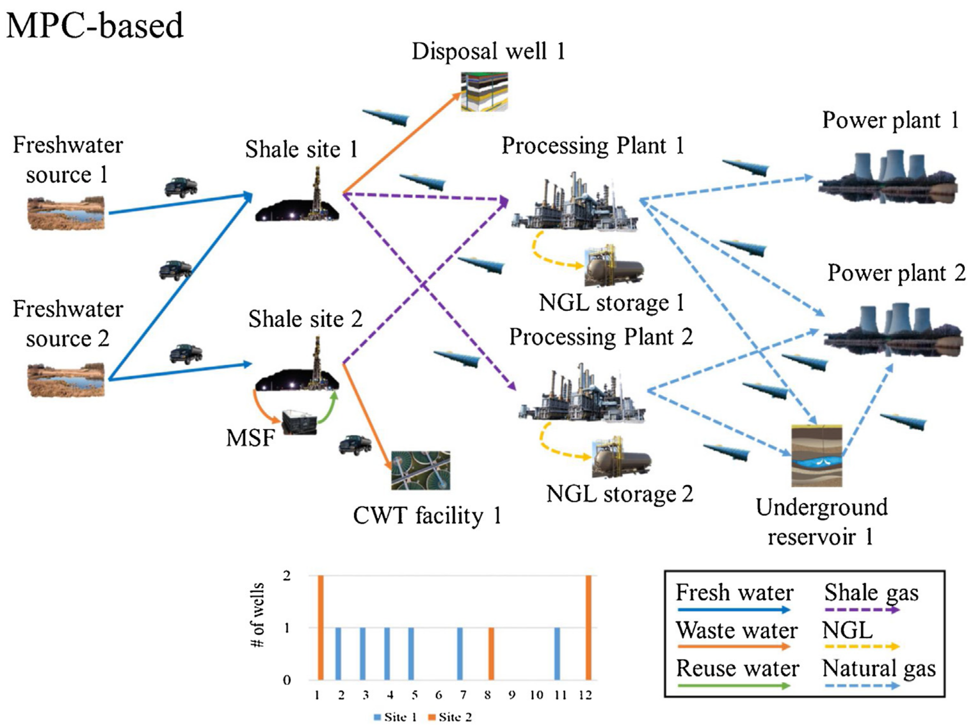

Fig. 8 – Optimal SGSCN configuration when the proposed MPC-based pumping schedule is used.

bbl) by trucks, and the freshwater to shale site 2 was supplied (995,492 bbl) from freshwater source 2 by a truck. When compared with the Nolte's pumping schedule case, a difference was shown in the wastewater treatment option. One MSF facility as onsite treatment facility, one CWT facility, and one disposal well were selected to handle the wastewater in the proposed MPC-based pumping schedule case. In shale site 1, the wastewater was transported (1,261,561 bbl) to the disposal well, and it was disposed in deep well without treatment. But, in shale site 2, some of the generated wastewater was reused in a nearby shale site by MSF facility (22,262 bbl), and the remaining wastewater (709,835 bbl) was transported to the CWT facility by a truck.

Like the Nolte's pumping schedule case, the eleven hydraulic fracturing jobs were completed to produce shale gas over three years from shale sites 1 (six wells) and 2 (five wells) with different pumping schedules. Two shale gas processing plants (1,500,000 msf per time period in processing plant 1 and 300,000 msf per time period in processing plant 2) were constructed with two NGL storage units. The amounts of electricity generated from power plants 1 and 2 are 2,033,137,345 MW h and 1,717,441,978 MW h, respectively. The details of the optimal SGSCN design when the proposed MPC-based pumping schedule is used are shown in Table 2.

5.2.3. *Optimal productions and storages of shale gas*

Although the total numbers of completed hydraulic fracturing jobs between the two cases were identical (eleven wells), the total amount of shale gas produced in the proposed MPC-based pumping schedule case (32.47×10^9 ft^3; Fig. 9b) is 7.98% higher than that of Nolte's pumping schedule case (30.07×10^9 ft^3; Fig. 9a); this is due to the fact that the final fracture geometry at the end of pumping, which significantly affects shale gas production, depends on the type of pumping schedules applied. A large amount of shale gas is produced right after a hydraulic fracturing job is completed, and the shale gas production rate decreases over time (shown in Fig. S1 and Table S1 in the ESI).

Appropriate hydraulic fracturing schedules have been determined to maximize the overall profit from the SGSCN (Fig. 9). After hydraulic fracturing is completed, most shale gas was produced in the early time period, and the production rate decreases rapidly over time. A rapid increase in the production rate at the 12th time period was due to the constraint that hydraulic fracturing jobs should be completed within 3 years.

For selling NGLs separated from natural gas at processing plants, NGLs can be stored in NGL storage units. Total storage amount of NGLs in the proposed MPC-based pumping schedule case (3.86×10^6 ft^3) was 7.52% higher than that of the Nolte's pumping schedule case (3.59×10^6 ft^3) (Fig. 10).

The NGL storage levels in both of the cases followed their shale gas production profiles (Fig. 9) because the amounts of separated NGLs are proportional to the shale gas produced from shale sites. Also, natural gas separated at processing plants can be stored in underground reservoirs before being sent to power plants to generate electricity, and the storage profiles of natural gas for both of the cases are shown in Fig. S2 in ESI.

Remark 5. We focus on the development of a novel framework that integrates the SGSCN model and the closed-loop operation of hydraulic fracturing. Once a final fracture geometry is achieved, shale gas production rate and the amounts of freshwater required and wastewater recovered in each shale were also calculated by CMG software and the empirical models, respectively. Compared to Nolte's pumping schedule which did not consider the fracture geometry, the amounts of freshwater required and wastewater recovered at each shale well were decreased in the closed-loop operation of hydraulic fracturing. Therefore, one of the key findings from this study is that the consideration of fracture geometry in hydraulic fracturing affects desired SGSCN configuration and operating

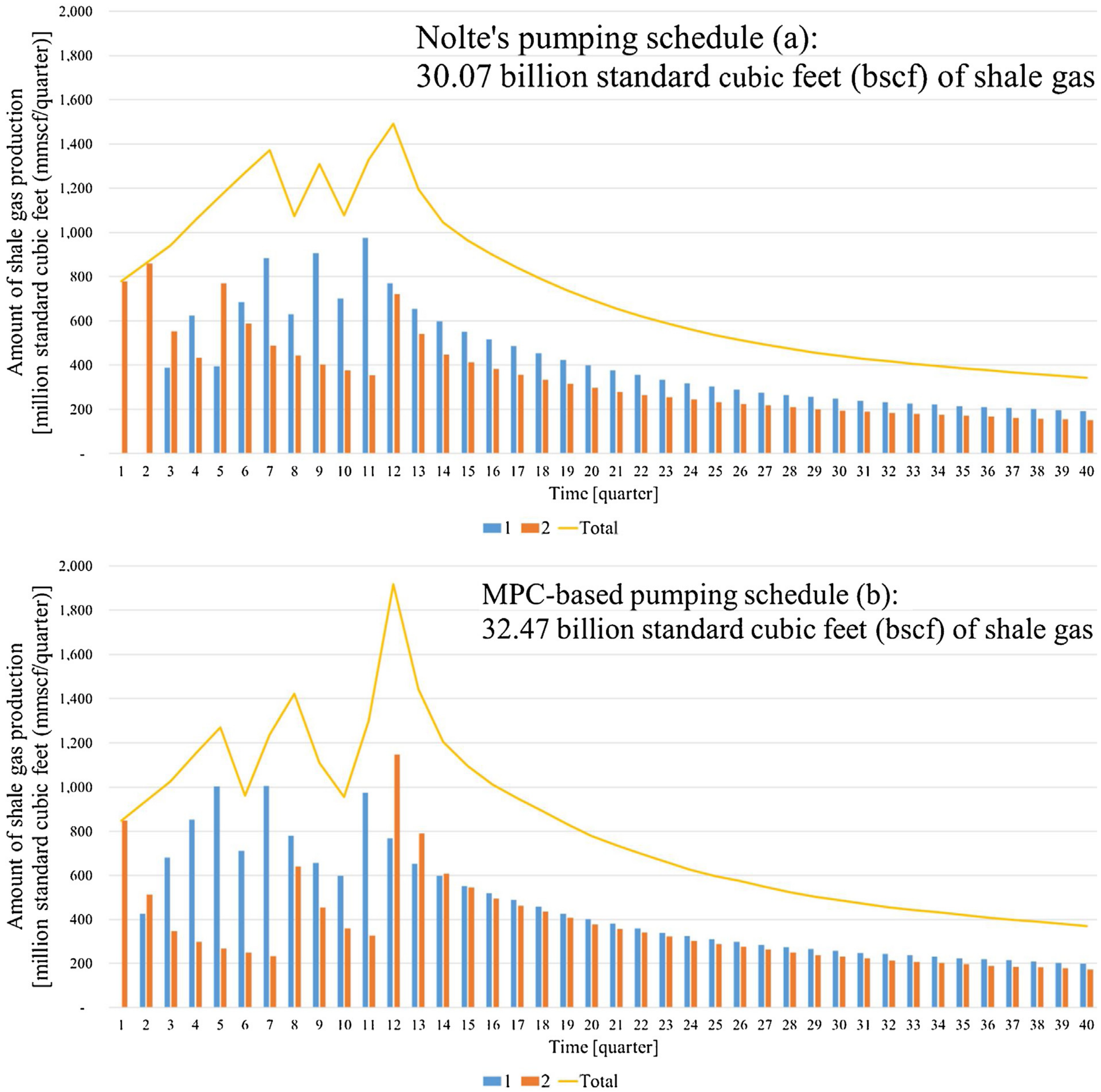

Fig. 9 – Optimal shale gas production profiles of the SGSCN when (a) Nolte's and (b) the proposed MPC-based pumping schedules are used.

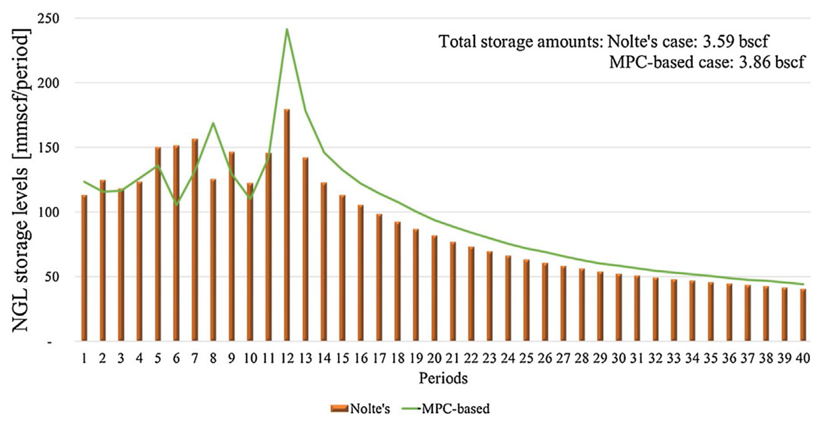

Fig. 10 – Optimal NGL storage profiles.

strategy, and applying the MPC-based pumping schedule of hydraulic fracturing was proven to be more profitable than Nolte's pumping schedule.

6. Conclusions

In this study, we focus on the development of a novel framework that integrates a MPC-based pumping schedule, proposed in our earlier work, and a SGSCN model. This framework allowed us to determine the optimal configuration that maximizes the overall profit of the SGSCN by taking into account the information available from the MPC-based pumping schedule, which includes the amounts of freshwater required, wastewater generated, and shale gas produced from the fractured wells. The proposed SGSCN design framework has been compared to the case when the mathematical model of SGSCN was integrated with a suboptimal pumping schedule like Nolte's pumping schedule. The overall profit of the former, which utilized the MPC-based pumping schedule, was 4.49% higher than that of the latter, which was designed on Nolte's pumping schedule. In this study, the total profit would be improved by integrating SGSCN model and the MPC-based pumping schedule of hydraulic fracturing as they achieve an optimal propped fracture geometry leading to a maximum shale gas production rate; however, there are some weaknesses such as no consideration of CO_2 emission and uncertain selling price of electricity. In the future, CO_2 emission and uncertainty in electricity selling price should be considered to evaluate the environmental impact and to handle the unexpected market conditions.

Acknowledgments

The authors gratefully acknowledge financial support from the National Science Foundation (CBET 1804407), Artie McFerrin Department of Chemical Engineering and the Texas A&M Energy Institute. The research was partially supported by Development of Platform for Future New Growth Engines CO2 High-Value Added Commercialization Program through Korea Institute for Advancement of Technology (KIAT) funded by the Ministry of Trade, Industry and Energy (no. 1415157630-R0006251).

Appendix A. Supplementary data

Supplementary material related to this article can be found, in the online version, at doi:https://doi.org/10.1016/j.cherd.2019.05.016.

References

Administration, U.E.I, 2011. Natural Gas Processing Plants in the United States: 2010 Update.

U.S. Energy Information Administration, Electric power monthly. https://www.eia.gov/electricity/monthly/epm_table_grapher.php?t=epmt_5_6_a. (Accessed 2 July 2019).

Ahn, Y.-C., Lee, I.-B., Lee, K.-H., Han, J.-H., 2015. Strategic planning design of microalgae biomass-to-biodiesel supply chain network: multi-period deterministic model. Appl. Energy 154, 528–542.

Allen, D.T., Torres, V.M., Thomas, J., Sullivan, D.W., Harrison, M., Hendler, A., Herndon, S.C., Kolb, C.E., Fraser, M.P., Hill, A.D., 2013. Measurements of methane emissions at natural gas production sites in the United States. Proc. Natl. Acad. Sci. 110, 17768–17773.

Al-Nory, M.T., Brodsky, A., Bozkaya, B., Graves, S.C., 2014. Desalination supply chain decision analysis and optimization. Desalination 347, 144–157.

Annevelink, M., Meesters, J., Hendriks, A., 2016. Environmental contamination due to shale gas development. Sci. Total Environ. 550, 431–438.

Bartholomew, T.V., Mauter, M.S., 2016. Multiobjective optimization model for minimizing cost and environmental impact in shale gas water and wastewater management. ACS Sustain. Chem. Eng. 4, 3728–3735.

Beamon, B.M., 1998. Supply chain design and analysis: models and methods. Int. J. Prod. Econ. 55, 281–294.

Bhattacharya, S., Nikolaou, M., Economides, M., 2012. Unified fracture design for very low permeability reservoirs. J. Nat. Gas Sci. Eng. 9, 184–195.

Cafaro, D.C., Grossmann, I.E., 2014. Strategic planning, design, and development of the shale gas supply chain network. AIChE J. 60, 2122–2142.

Chebeir, J., Geraili, A., Romagnoli, J., 2017. Development of shale gas supply chain network under market uncertainties. Energies 10, 246.

Chen, Y., He, L., Li, J., Zhang, S., 2018. Multi-criteria design of shale-gas–water supply chains and production systems towards optimal life cycle economics and greenhouse gas emissions under uncertainty. Comput. Chem. Eng. 109, 216–235.

Cipolla, C., Lolon, E., Mayerhofer, M., 2009. The Effect of Proppant Distribution and Un-Propped Fracture Conductivity on Well Performance in Unconventional Gas Reservoirs. SPE, 119368.

Cost, L., 2014. Levelized Avoided Cost of New Generation Resources in the Annual Energy Outlook 2014. US Energy Information Administration.

Economides, M.J., Demarchos, A.S., 2008. Benefits of a p-3D over a 2D model for unified fracture design. SPE International Symposium and Exhibition on Formation Damage Control.

Economides, M.J., Nolte, K.G., 1989. Reservoir Stimulation. Prentice Hall Englewood Cliffs, NJ.

Etoughe, P., Siddhamshetty, P., Cao, K., Mukherjee, R., Kwon, J.S.-I., 2018. Incorporation of sustainability in process control of hydraulic fracturing in unconventional reservoirs. Chem. Eng. Res. Des. 139, 62–76.

Gao, J., You, F., 2015a. Optimal design and operations of supply chain networks for water management in shale gas production: MILFP model and algorithms for the water-energy nexus. AIChE J. 61, 1184–1208.

Gao, J., You, F., 2015b. Shale gas supply chain design and operations toward better economic and life cycle environmental performance: MINLP model and global optimization algorithm. ACS Sustain. Chem. Eng. 3, 1282–1291.

Gao, J., You, F., 2015c. Stochastic programming approach to optimal design and operations of shale gas supply chain under uncertainty. In: 2015 IEEE 54th Annual Conference on Decision and Control (CDC). IEEE., pp. 6656–6661.

Gu, Q., Hoo, K.A., 2014. Evaluating the performance of a fracturing treatment design. Ind. Eng. Chem. Res. 53, 10491–10503.

Guerra, O.J., Calderón, A.J., Papageorgiou, L.G., Siirola, J.J., Reklaitis, G.V., 2016. An optimization framework for the integration of water management and shale gas supply chain design. Comput. Chem. Eng. 92, 230–255.

Hayes, T., 2009. Sampling and Analysis of Water Streams Associated with the Development of Marcellus Shale Gas. Marcellus Shale Initiat. Publ. Database.

He, C., You, F., 2014. Shale gas processing integrated with ethylene production: novel process designs, exergy analysis, and techno-economic analysis. Ind. Eng. Chem. Res. 53, 11442–11459.

Horner, P., Halldorson, B., Slutz, J.A., 2011. Shale gas water treatment value chain—a review of technologies, including case studies. SPE Annual Technical Conference and Exhibition.

Howarth, R.W., Santoro, R., Ingraffea, A., 2011. Methane and the greenhouse-gas footprint of natural gas from shale formations. Clim. Change 106, 679.

Jang, E., Jeong, S., Chung, E., 2017. Application of three different water treatment technologies to shale gas produced water. Geosyst. Eng. 20, 104–110.

Kargbo, D.M., Wilhelm, R.G., Campbell, D.J., 2010. Natural Gas Plays in the Marcellus Shale: Challenges and Potential Opportunities. ACS Publications.

Kumar, G., Shobana, S., Chen, W.-H., Bach, Q.-V., Kim, S.-H., Atabani, A., Chang, J.-S., 2017. A review of thermochemical conversion of microalgal biomass for biofuels: chemistry and processes. Green Chem. 19, 44–67.

Ladlee, J., Jacquet, J., 2011. The implications of multi-well pads in the Marcellus Shale.

Lira-Barragán, L.F., Ponce-Ortega, J.M., Guillén-Gosálbez, G., El-Halwagi, M.M., 2016. Optimal water management under uncertainty for shale gas production. Ind. Eng. Chem. Res. 55, 1322–1335.

Liu, S., Valkó, P.P., 2017. Optimization of spacing and penetration ratio for infinite-conductivity fractures in unconventional reservoirs: a section-based approach. SPE J. 22, 1877–1892.

Lutz, B.D., Lewis, A.N., Doyle, M.W., 2013. Generation, transport, and disposal of wastewater associated with Marcellus Shale gas development. Water Resour. Res. 49, 647–656.

Narasingam, A., Kwon, J.S.-I., 2017. Development of local dynamic mode decomposition with control: application to model predictive control of hydraulic fracturing. Comput. Chem. Eng. 106, 501–511.

Narasingam, A., Siddhamshetty, P., Kwon, J.S.-I., 2017. Temporal clustering for order reduction of nonlinear parabolic PDE systems with time-dependent spatial domains: application to a hydraulic fracturing process. AIChE J. 63, 3818–3831.

Narasingam, A., Siddhamshetty, P., Kwon, J.S.-I., 2018. Handling spatial heterogeneity in reservoir parameters using proper orthogonal decomposition based ensemble Kalman filter for model-based feedback control of hydraulic fracturing. Ind. Eng. Chem. Res. 57, 3977–3989.

Nolte, K., 1986. Determination of proppant and fluid schedules from fracturing-pressure decline. SPE Prod. Eng. 1, 255–265.

Olmstead, S.M., Muehlenbachs, L.A., Shih, J.-S., Chu, Z., Krupnick, A.J., 2013. Shale gas development impacts on surface water quality in Pennsylvania. Proc. Natl. Acad. Sci. 110 (13), 4962–4967, 201213871.

Paltsev, S., Jacoby, H.D., Reilly, J.M., Ejaz, Q.J., Morris, J., O'Sullivan, F., Rausch, S., Winchester, N., Kragha, O., 2011. The future of US natural gas production, use, and trade. Energy Policy 39, 5309–5321.

Raluy, G., Serra, L., Uche, J., 2006. Life cycle assessment of MSF, MED and RO desalination technologies. Energy 31, 2361–2372.

Siddhamshetty, P., Kwon, J.S.I., Liu, S., Valkó, P.P., 2018a. Feedback control of proppant bank heights during hydraulic fracturing for enhanced productivity in shale formations. AIChE J. 64, 1638–1650.

Siddhamshetty, P., Wu, K., Kwon, J.S.-I., 2018b. Optimization of simultaneously propagating multiple fractures in hydraulic fracturing to achieve uniform growth using data-based model reduction. Chem. Eng. Res. Des. 136, 675–686.

Siddhamshetty, P., Yang, S., Kwon, J.S.-I., 2018c. Modeling of hydraulic fracturing and designing of online pumping schedules to achieve uniform proppant concentration in conventional oil reservoirs. Comput. Chem. Eng. 114, 306–317.

Siddhamshetty, P., Wu, K., Kwon, J.S.-I., 2019. Modeling and control of proppant distribution of multi-stage hydraulic fracturing in horizontal shale wells. Ind. Eng. Chem. Res. 58, 3159–3169.

Singh Sidhu, H., Siddhamshetty, P., Kwon, J., 2018. Approximate dynamic programming based control of proppant concentration in hydraulic fracturing. Mathematics 6, 132.

Slutz, J.A., Anderson, J.A., Broderick, R., Horner, P.H., 2012. Key shale gas water management strategies: an economic assessment. International Conference on Health, Safety and Environment in Oil and Gas Exploration and Production.

Van der Bruggen, B., Vandecasteele, C., 2002. Distillation vs. membrane filtration: overview of process evolutions in seawater desalination. Desalination 143, 207–218.

Wang, Q., Chen, X., Jha, A.N., Rogers, H., 2014. Natural gas from shale formation—the evolution, evidences and challenges of shale gas revolution in United States. Renew. Sustain. Energy Rev. 30, 1–28.

Weber, C.L., Clavin, C., 2012. Life cycle carbon footprint of shale gas: review of evidence and implications. Environ. Sci. Technol. 46, 5688–5695.

Wilson, J.M., VanBriesen, J.M., 2012. Oil and gas produced water management and surface drinking water sources in Pennsylvania. Environ. Pract. 14, 288–300.

Yang, L., Grossmann, I.E., Manno, J., 2014. Optimization models for shale gas water management. AIChE J. 60, 3490–3501.

Yang, S., Siddhamshetty, P., Kwon, J.S.-I., 2017. Optimal pumping schedule design to achieve a uniform proppant concentration level in hydraulic fracturing. Comput. Chem. Eng. 101, 138–147.